# PRECISE CHARACTERIZATION OF SOFT-MAGNETIC MATERIALS AT HIGH SATURATION

Gorazd Modrijan, Marko Petkovšek, Peter Zajec, Danijel Vončina

University of Ljubljana, Faculty of Electrical Engineering, Ljubljana, Slovenia

**Key words:** ring core, soft-magnetic material, measuring system, DSP, low-distortion, form factor, B-H curve

**Abstract:** The presented paper deals with a computerized measuring system for evaluating magnetic properties of soft-magnetic ring cores (in compliance with the IEC60404-2 standard). A measuring set-up with a feedback power amplifier is introduced. Its basic operation is explained and an upgraded version is presented. Its main feature is a superior control loop based on a repetitive action control method which assures an accurate and stable secondary induced sinusoidal voltage waveform without voltage zero-crossing distortion caused by a large magnetizing current. Two variants of the repetitive method are presented which provide more realistic measurements of magnetic field strength *H* at the specified amplitude of the secondary induced voltage. Measurements done without and with the repetitive action corrector are presented and discussed. Reasons for choosing one variant are given and results that confirm the improvement over a conventional approach without the repetitive controller are shown.

# Merjenje lastnosti mehkomagnetnih materialov pri visoki stopnji magnetnega nasičenja

**Ključne besede:** toroidno jedro, mehkomagnetni material, merilni sistem, DSP, nizko popačenje, faktor oblike, B-H krivulja

**Izvleček:** V članku je predstavljen mikrokrmilniško nadzorovan merilni sistem za merjenje parametrov mehkomagnetnih jeder z zaključeno magnetno potjo (po predpisih, ki jih določa standard IEC60404-2). Opisano je osnovno merilno vezje, ki temelji na linearnem močnostnem ojačevalniku z negativno povratno zanko. Razloženi so temelji njegovega delovanja. Predlagana je nadgradnja merilnega sistema z nadrejeno regulacijsko zanko z regulatorjem, ki temelji na repetitivni korekcijski metodi. Slednji je posebno primeren za zagotavljanje stabilne sinusne oblike sekundarne inducirane napetosti brez popačenja pri prehodu skozi ničlo, ki ga povzroča velik magnetilni tok. Predstavljeni sta dve različici repetitivne korekcijske metode, ki omogočata realnejše posredno merjenje magnetne poljske jakosti *H*. Obe različici učinkovito zmanjšujeta konico magnetilnega toka ter posledično magnetne poljske jakosti, pri tem pa ohranjata amplitudo sekundarne inducirane napetosti nespremenjeno. Predstavljene so primerjalne meritve, opravljene na opisanem merilnem vezju brez in z uporabo nadrejene regulacijske zanke z repetitivnim regulatorjem. Podani so razlogi za izbiro ene od izvedb ter pridobljeni rezultati. Opravljene meritve potrjujejo izboljšave, ki jih doprinese regulirani sistem v primerjavi z nereguliranim.

## Introduction

In the field of soft-magnetic cores manufacturing the measurement of magnetic field strength *H* at a predefined magnetic flux density *B* is of outmost importance to determine the quality of assembled magnetic cores. The measurement deviations, set by the standards regulating this field /1 - 2/, are relatively tolerant and allow various methods or power supply assemblies for achieving them. Nonetheless, the common denominator of all such devices is that they should keep the secondary induced voltage waveform sinusoidal even when the device under test (D.U.T.) requires high flux density. Such a device should be able to:

- perform B-H curve measurement of soft-magnetic cores which are used in low and medium- frequency applications such as voltage and current transformers, yokes for motors or line filters,
- perform hysteresis loss measurement, which is crucial for minimizing core losses and so enabling reduction in size of magnetic devices.

The accurate measurement of magnetic field strength *H* becomes especially important when estimating cores that are measured in high saturation region. A couple percents deviation of the measured value from the actual value can mean all the difference when considering the material to choose.

To obtain magnetic parameters of soft-magnetic materials, measurements are usually done using standard 25 cm (Epstein) test core assemblies /3 - 5/ consisting of several steel strips. In practice, however, it is desired to perform magnetic measurements not only on magnetic strips, but also to perform production quality control tests on ring cores after they have been assembled /6/.

The standards that regulate the field of magnetic measurements demand a secondary induced voltage of stable amplitude and accurate shape. During measurements, the voltage and frequency variations should not exceed ± 0.2 % of the required value. For the determination of:

- the specific total losses,
- the specific apparent power and
- the *rms* value of the magnetic field strength,

the form factor $FF_U$ (which is the ratio of the *rms* value of the signal to its average rectified value) of the secondary voltage $u_S$ must be maintained in a range of 1.111 ± 1% otherwise the above measurements (and other derivate quantities) are not valid. The given requirements can be

met in two different ways: solely with a feedback power amplifier and by using a superior digital control loop. Both cases are presented in this paper.

## Theory

Parameters of a soft-magnetic ring core are usually measured in a well known measurement set-up, where the D.U.T. is magnetized by an alternating primary current $i_P$, causing a magnetic field strength /2/:

$$H = i_P \cdot N_P / l_{FE}, \quad (1)$$

where $N_P$ is the number of primary turns and $l_{FE}$ the effective magnetic path of the D.U.T., which can be calculated from the dimensions (the outer and inner ring diameters) of the ring core. As a consequence of the magnetic flux density $B$, voltage is induced in a secondary winding:

$$u_S = - N_S \cdot S_{FE} \cdot dB / dt, \quad (2)$$

where $N_S$ and $S_{FE}$ stand for a number of secondary turns and cross-sectional area of the D.U.T., respectively.

To minimize the impact of the shape of the primary current $i_P$ to the measurement of the specific apparent power and the *rms* value of $H$, the international standard implies that the measurement should be made with a sinusoidal magnetic polarization $B$ /1, 2/. In this case, the *rms* value of the induced voltage $u_S$, becomes proportional to the maximum value of $B$:

$$U_S = 4.44 \cdot \hat{B} \cdot f \cdot S_{FE} \cdot N_S, \quad (3)$$

where $f$ is the frequency of the induced voltage.

The main problem when measuring a B-H curve is actually the deviation of the secondary induced voltage (or magnetic flux density $B$) from an ideal sinusoidal waveform, which is caused by a high (peak) current flowing when the soft-magnetic core is in a magnetic saturation. A deformed secondary induced voltage yields a higher peak current and consecutively declines the secondary voltage waveform from the optimal one, so corrupting the measurement of magnetic field strength. By correcting the shape of the induced voltage $u_S$, the peak current can be diminished and measurement of $H$ improved!

## System Description

One possible method to fulfill the required voltage shape criteria ($FF_U$) involves a power amplifier with an attached primary winding of the D.U.T. to its output, while the secondary voltage is fed back to its negative input in order to instantaneously control the secondary voltage waveform (Figure 1).

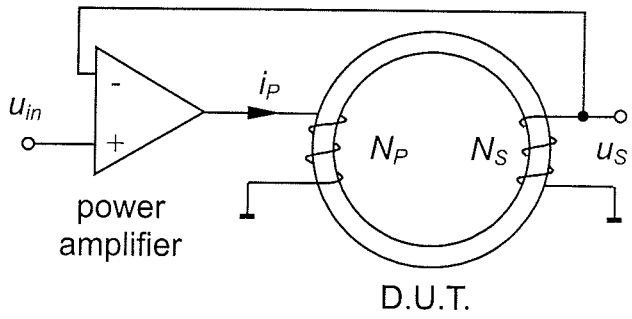


*Figure 1: Principle of the power amplifier assisted measurement set-up*

The voltage drop in the primary winding of the above set-up is compensated through the control of a power amplifier. Unfortunately, the DC offset voltage of the power amplifier (resulting in the pre-magnetized magnetic core) causes incorrect measurement results. Another potential problem is the power amplifier instability appearing at low impedance loads.

The problem of DC offset voltage can be successfully solved with the measurement set-up shown in Figure 2 /7/. Its main idea is to use an additional matching transformer (Tr.) placed between the power amplifier (PA) and the D.U.T. The matching transformer prevents the D.U.T. from being pre-magnetized with the remaining DC voltage offset at the PA output, which is left uncompensated through the use of a low-pass (LP) filter ($f_C$ = 2 Hz). Since the transformer is a part of the control loop, no special requirements have to be met during its design stage, except that the possible pre-magnetization has to be taken into consideration. To keep the matching transformer size in reasonable limits, the primary feedback loop of the PA is upgraded with a low-pass filter. Due to its low cut-off frequency, it forces only the DC component of the PA output voltage into the summation point, thus reducing the DC pre-magnetization of the D.U.T. In addition, the matching transformer with a proper turn ratio adjusts the low impedance of the device's primary winding to the PA and therefore provides its nominal burden in spite of the primary turns $N_P$ as well as secondary turns $N_S$ reduction.

A request for the measurement set-up is that it must cover a wide range of ring core assortments with the possibility of the secondary voltage as well as primary magnetizing current swinging in wide dynamic ranges. Attempts to fulfill this demand can lead to PA instability or to measurement inaccuracy due to the insufficient signal to noise ratio. In order to raise the measurement accuracy, depending basically on the sensitivity of the magnetic flux evaluation that is obtained by means of numerical integration of the induced secondary voltage /3/, and expand the measurement range, programmable gain amplifiers (PGA) were installed in both measurement paths terminated with 12-bit analog-to-digital converters (ADCs) as well as in the negative feedback control loop.

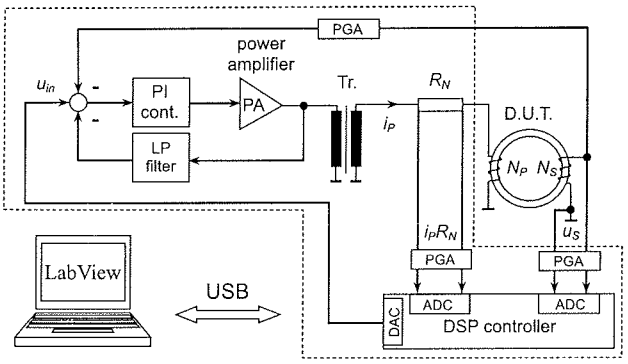


*Figure 2: The proposed experimental set-up*

Upon the given core data (outer diameter (O.D.), inner diameter (I.D.), height (H) and filling factor) and the preferred magnetization level, the appropriate gain is set by a digital signal processor (DSP). The same DSP also cares for data capturing and the generation of a sinusoidal reference voltage $u_{in}$.

Because the described system already comprises a DSP controller, an additional superior control loop is implemented in it, which further improves the overall accuracy of the secondary induced voltage $u_S$.

## Superior Control Loop Design

The superior control of the described system is comprised of two successive controllers which are not active at the same time. The first is an I-like fuzzy logic controller (FLC) which oversees the magnitude of the reference voltage $u_{in}$ necessary to achieve the desired amplitude of the induced secondary voltage $u_S$. It is activated every time the reference voltage is changed and deactivated when the secondary voltage $u_S$ reaches the desired value. The second controller (enabled when the FLC is deactivated) is based on a repetitive (integral) action method which corrects the shape of the generated reference signal $u_{in}$ in order to achieve a sinusoidal induced secondary voltage with a *THD* as low as possible. The requirement for minimal *THD* is a consequence of the desired form factor $FF_U$. The corrector basically adds a correction waveform $u_{cor}$ to the sine reference voltage effectively forming the input waveform $u_{in}'$.

## Fuzzy Logic Controller

Because of the design of the system it is impossible to accurately predict the amplitude of the secondary induced voltage in relation to the voltage applied on the primary winding. This is made worse by the DSP not knowing what kind of soft-magnetic material is being analyzed. The only known fact is that the ratio of the secondary induced voltage to the primary applied voltage ($\kappa$) varies from almost 1 to approximately 0.8, in dependence of the D.U.T., number of primary and secondary winding turns and gain factor of the power amplifier's feedback control loop.

Because of stated reasons behind the uncertainty of the amplitude of secondary voltage an I-like FLC is used to control the amplitude of the primary voltage $u_{in}$. There are two demands it must fulfill:

- it must convey the secondary induced voltage to its predestined value in at least ten periods and
- it must not overshoot.

The first demand is based on the maximum measurement time allowed, while the second is inherent of the measurement method itself: because the D.U.T. is in an unknown state (usually pre-magnetized) it must be demagnetized before the first measurement could take place. This is achieved by bringing the device close to saturation and then back down to zero. The problem arises if/when the D.U.T. enters deep into the saturation region and the current exceeds all anticipated values. At this point the induced secondary voltage is not sinusoidal any more and amplitude measurement/calculation becomes impossible thus hindering the functioning of the FLC.

The I-like FLC is of SISO type: the (single) input is the degree of deviation of the amplitude of the secondary induced voltage $u_S$ from the desired value $u_{Sref}$ (which is an internal DSP value send by the PC). The deviation is calculated as:

$$e = u_{Sref} - u_S, \tag{4}$$

where:

$$u_S = \kappa \cdot u_{in}. \tag{5}$$

The (single) output of the FLC ($u_{in}$) is the scaled (internal) sinusoidal reference waveform $u_{ref}$:

$$u_{in} = \alpha \cdot u_{ref}. \tag{6}$$

The gain $\alpha$ of the I-like FLC is altered until the voltage $u_{in}$ produces the desired secondary induced voltage $u_S$ ($e = 0$) in which case the attenuation of the system $\kappa$ is completely compensated.

The action of the FLC is divided in dependence of the error $e$ in four regions: L, M, S and Z. If the deviation $e$ is very large (region L), the increase (or decrease) of the reference voltage $u_{in}$ is large (meaning a small integral constant) and if the deviation is small (region S), the increase (or decrease) of the reference voltage is small (large integral constant). When the amplitude of the secondary induced voltage coincides with the desired value, the FLC sets the integral constant to zero and so effectively disabling itself and starting the repetitive action controller (see next chapter).

The cross points of the five regions are calculated from the known parameters of the source and the D.U.T. and their values are set to bring the secondary voltage to its final value in about ten periods. The initial integral constant of the FLC is calculated approximately and is chosen in a way to cause a change of secondary voltage of not less then about 12.5 % (taking into account an approximation of the

system attenuation). All the subsequent incrementations (or decrementations) can be only equal to or smaller than the initial value.

## Repetitive Control Method

The proposed control method for the pertinent system is a variant of a repetitive action control method /8/, which is especially suitable for correcting periodic signals (of voltage and/or current). In the past, repetitive control methods have seen extensive application where correction of a periodic waveform is required /9 - 12/ (e.g. motor control applications and PWM switching power supplies like UPS devices), mainly because of their reliable operation, low cost and ease of implementation. In our case, we chose an integral repetitive action control method since the output waveform of the amplifier and the disturbance are always periodic, even when a nonlinear load is supplied by the voltage power amplifier /8, 13/. The control principle moreover does not depend on internal control loops of the voltage power amplifier nor does it require any special knowledge about its parameters. Besides the periodic occurrence of disturbances, the only condition that must be met for the implementation of the control principle is the stability of the amplifier.

A simplified representation of the voltage power source is shown in Figure 3. The periodic disturbances causing output voltage distortions are summarized in a load-dependent disturbance signal $d$, which is chosen intentionally to simplify the analysis. It is especially appropriate when analyzing the impact of periodic disturbances and nonlinear distortion of output voltage of a power supply with a nonlinear load.

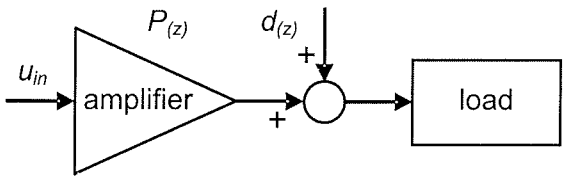


*Figure 3: Described system in z domain with disturbance signal d.*

Regardless of the type of repetitive control mechanism, they all rely on operation of a discrete number of period-based correctors. Figure 4 shows a plug-in repetitive controller /14/ processing the error $\varepsilon$, which is (at least in the first correction period) the difference between the input reference waveform $u_{in}$ and the actual output waveform $u_S$. The calculated and stored values of the error $\varepsilon_{(n,T)}$ are used to form a periodical correction waveform $u_{cor}$, which is added to the original (in most cases a sine wave) reference waveform $u_{in}$, thus effectively reducing the error of the output waveform of the amplifier/compensating the disturbance $d$.

The basic idea of the repetitive controller is that a period $T$ of the reference (and sampled output) voltage is divided in $N$ discrete intervals of duration $\tau$ (where $T = N \cdot \tau$). In each interval $n$, the acquired sample of the amplifier output voltage $u_{S(n,T)}$ is subtracted from the reference value $u_{in(n)}$. The calculated error $\varepsilon_{(n,T)}$ at the present discrete interval $n$ in a particular period $T$ is then stored twice: unmodified in a table of correction values (which has $N$ different positions) at the position corresponding to the discrete interval $n$, and scaled by $G_{(z)}$ in a second correction table (with $N$ positions) at position $n$ too. The same procedure is applied to all the intervals in a given period of the generated waveform.

In the next period ($T + 1$), the unmodified value of the error of a particular interval $n$ (of the previous period) is scaled by the factor $K_r$ and added to the other (already scaled) value of error of the previous period interval $n$. The sum of both values form a quant of the correction waveform:

$$u_{cor(n,T)} = K_r \cdot \varepsilon_{(n,T)} + \sum_{i=0}^{i=T} G_{(z)} \cdot \varepsilon_{(n,i)}, \qquad (7)$$

which is summed up to the reference voltage $u_{in(n)}$ and the result is a new input waveform:

$$u_{in}'_{(n,T+1)} = u_{in(n)} + u_{cor(n,T)}. \qquad (8)$$

The output voltage $u_{S(n,T+1)}$ of the amplifier is meanwhile sampled again and the new error $\varepsilon_{(n,T+1)}$ in a specific interval is recalculated. It is stored unmodified in the first table and scaled by $G_{(z)}$, summed to the previously scaled and stored error $\varepsilon_{(n,T)}$ of the $n$-th interval and stored again at the corresponding position in the (second) table of correction values for subsequent use in the following period ($T + 2$).

Owing to the repeating execution of the correction procedure, the (second) table of scaled errors contains the sums of all past errors $\varepsilon_{(n)}$ of all specific correction intervals $n$ independently. Consequently, the correction waveform

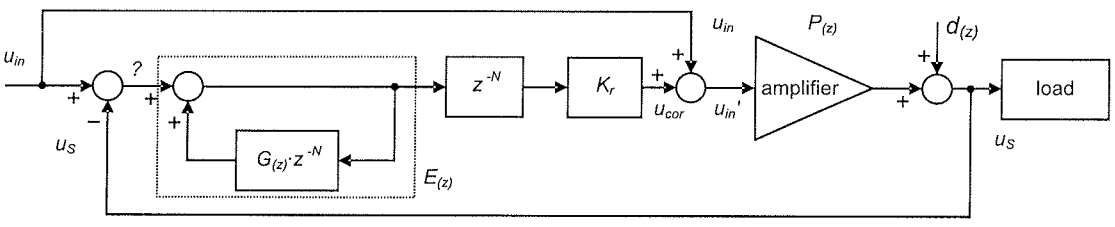


*Figure 4: Block diagram of a classic repetitive action control method in z domain.*

$u_{cor(n,T)}$ behaves as if it is formed with the help of $N$ correctors, each correcting the value of one interval $n$. Due to the nature of the control method, a sub-cycle response is impossible, meaning that the error detected in a certain period can be suppressed at best in the following period.

Figure 4 shows a block diagram of the described control method in $z$ domain, where the time delay unit $z^{-N}$ delays the computed correction waveform for one entire period $T$ (composed of $N$ samples). Similarly, a time delay unit $z^{-1}$ delays the execution for one sample. The key element of the repetitive action controller is the inner loop with the internal model $G_{(z)} \cdot z^{-N}$. Its closed loop transfer function is:

$$E_{(z)} = \frac{1}{1 - G_{(z)} \cdot z^{-N}}, \qquad (9)$$

where $G_{(z)}$ can be a constant or a function of $z$, e.g. a low-pass filter /15/ or a second order filter. In the time domain, this internal model is an integrator (if $G_{(z)} = 1$) summing up the error $\varepsilon$ of the $n$-th correction interval from the first to all successive periods. As explained before, this sum is used to correct the $n$-th interval of the reference waveform.

While the implemented correction method was tried out and found to be good, at some point it aroused concerns linked with the usage of data memory space of the DSP in which the calculations where executed. Consecutively, a modified version of the correction method was implemented (Figure 5), which required one memory table less then the previous method and had some other modifications:

- the function $G_{(z)}$ of the closed loop model $I_{(z)}$ was chosen to be/set to one so effectively making the closed loop model $I_{(z)}$ a proper integrator,
- an additional proportional model $Q$, used before the closed loop model $I_{(z)}$ was introduced, which regulates the export of the error $\varepsilon$ which is added to the already stored errors,
- the constant $K_I$ was dropped,
- two time advance units ($z^q$ and $z^h$) were added.

Although it was later found out, that the memory concerns were groundless, the correction method was retained. Its advantages were shorter calculation time and reduced data memory usage while having better stability and roughly the same ability to suppress waveform distortions (or lower *THD*).

## Repetitive Action Control Method Implementation

Both described control methods (classic and adapted) were implemented in the described B-H analyzer and tested. They work well, although with some distinctions in speed and accuracy. While the first is a little better in terms of the ability to reduce *THD*, the second allows for a wider deviation of the parameters of the regulator from the optimal value with minimal deterioration of *THD*.

The reference signal $u_{in}$ in both implementations consists of 1000 samples per period. This was also the sampling rate of the AD converter, meaning that the correction waveform $u_{cor}$ is also formed of the same number of intervals. Taking into account the Nyquist theorem, frequencies up to 50 kHz were sampled and corrected.

The implemented correction method has also two time advance units:

- $z^q$ in the direct path, which is used for correcting the various time delays (caused by the sampling time of the ADC, the conversion time of the digital-to-analog converter (DAC) and other time delays) and without which the actual realization of the correction method would not work,
- $z^h$ in the feedback branch, which implementation is not necessarily required, but it is useful to reduce the amplitude of the correction waveform $u_{cor}$ caused by the phase shift between the input and output of the system.

## Measurements

All the following measurements were made on an experimental model of the described B-H analyzer. The frequency domain analyses were made by means of a dynamic signal analyzer HP35665A. The measured frequency range was 0 to 3.2 kHz and a flat top windowing method was selected. For the *THD* calculation the harmonic components up to the 64$^{th}$ were observed and averaged over 30 measurements. The D.U.T. was a thin metal M0 silicon-iron toroidal core O.D./I.D./H.: 53/39/18 mm with two primary and two secondary winding turns.

Figure 6 shows test conditions without and with the repetitive action control method enabled and after the desired value of the secondary voltage amplitude has been set by

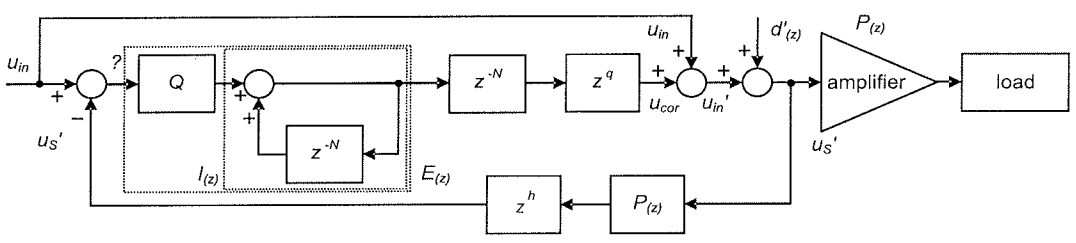


*Figure 5: Block diagram of the implemented repetitive action control method in z domain.*

the FLC. Shown are the secondary induced voltages, which are proportional to magnetic flux density $B$ (3), and currents, which are proportional to magnetic field strength $H$ (1). The voltage waveform $u_{Scor}$ is shifted up by 0.2 of a division because off a better visual distinction from the $u_S$ waveform, while currents $i_P$ are not.

The voltage was set to 120 mV peak, which for the D.U.T. corresponds to a magnetic flux density of 1.600 T. The D.U.T. was clearly in magnetic saturation. In the case of uncorrected secondary voltage the calculated form factor $FF_U$ was 1,113 % (which is well within the parameters prescribed by the standard). The effective value of magnetic field strength in this instance was 28.3 A/m.

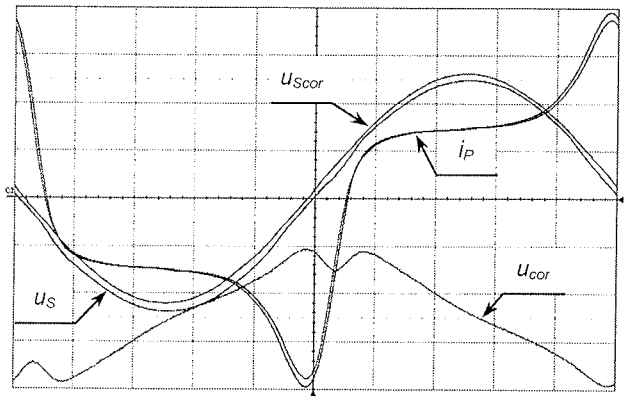


*Figure 6: Secondary voltages* $u_S$, *corrected secondary voltage* $u_{Scor}$, *primary currents* $i_P$ *and correction waveform* $u_{cor}$ *(*$k_{Us}$ *= 200 mV/div,* $k_{ip}$ *= 2 A/div,* $k_{Ucor}$ *= 2 mV/div,* $t$ *= 2 ms/div)*

In the second case, with the correction enabled and the same reference magnetic flux density, the calculated form factor was 1.1108 %. The measured effective value of magnetic field strength was 27.7 A/m. From the given values we can calculate, that a 0.2 % change in the form factor contributes to a 2.16 % decrease in the magnetic field strength.

Figure 6 shows also a fifth signal which is the correction waveform $u_{cor}$ needed to achieve the low-distortion secondary induced voltage $u_{Scor}$. The waveform is again shifted down by 2.5 divisions because of clarity.

Both secondary voltage waveforms were analyzed in the frequency domain and their relative frequency spectra are shown in Figures 7 and 8. The first figure shows the frequency spectrum of the uncorrected and corrected voltage waveform of Figure 6 when the gain factor ($Z$) of the power amplifier's feedback loop was set to 1. The gray curve is the frequency spectra of the uncorrected voltage $u_S$. The measured *THD* is about 1.656 % and it was caused mainly by odd higher harmonics components between the 3rd and the 23rd. The black curve represents the conditions of the corrected system. The measured *THD* was 0.04 %. A slighter increase in the 52th and 53th higher harmonics can be observed which were preliminary absent.

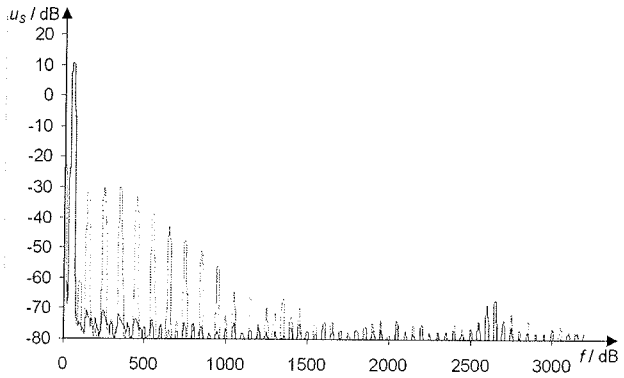


*Figure 7: Frequency spectrum of an uncorrected and corrected system (Z = 1)*

Another set of the same measurements was done, but with the gain of the power amplifier's feedback loop ($Z$) set to 4. The *THD* was in overall lower: 0.408 % with the correction disabled and 0.017 % with the correction enabled.

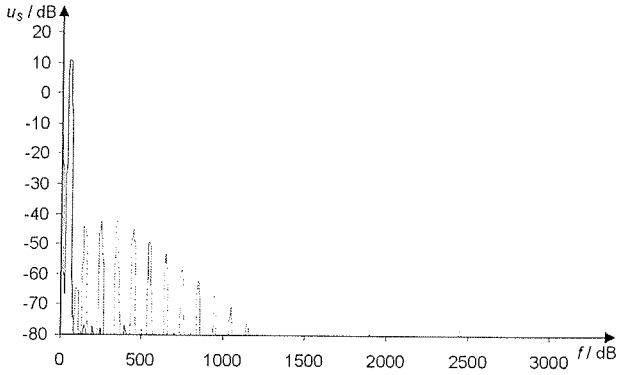


*Figure 8: Frequency spectrum of an uncorrected and corrected system (Z = 4)*

As can be seen from the figure above, the use of the gain factor in the power amplifier's feedback loop can greatly improve the *THD* factor because it forces a larger input voltage $u_{in}$, which can be set with greater accuracy. On the other hand, the gain factor must be used with care because of system stability concerns.

The following figure shows a B-H curve of the D.U.T. used for the presented measurements measured with the described system and with the repetitive action controller enabled.

As stated before, the same measurements were also done on a system controlled with a classical correction method (as seen in Figure 4). The acquired figures are not recorded in this paper because they deviate only minimally from the already presented. The measured form factor was the same while the calculated *THD* with correction enabled was actually a bit better: 0.016 %.

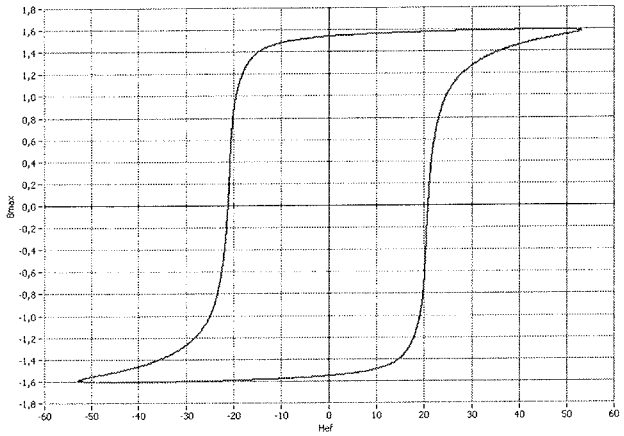


*Figure 9: B-H curve of the D.U.T.*

## Conclusion

The aim of the presented paper was the comparison between an uncorrected measurement set-up suitable for measuring magnetic field strength *H*, which was based on a feedback power amplifier and was already compliant with the tolerances imposed by the standard defining magnetic measurements, with the same supply set-up, but upgraded with a superior digital control loop. Two repetitive action control methods were implemented. Their goal was to achieve a better, more faithful reproduction of a sinusoidal waveform secondary induced voltage.

The first tested was a classical repetitive action correction method. Its use proved to be very effective in reducing the *THD* level of the secondary induced voltage $u_S$. The drawback was the fine tuning of parameters that it required for achieving the best results and possible problems with system stability if they were mismatched.

The second correction method was a modified version of the previous one, which required less parameters optimization. It yielded slightly worse error correction (greater *THD*), but it was much more robust. Nonetheless, the achieved results of form factor improvement were very good and at the end it was the chosen one because of ease of implementation and usage. The slightly greater *THD* it produced was so small, thet it did not weigh up its other advantages.

With the use of the repetitive action control method improvement on magnetic field strength *H* measurements are more than perceivable. Although a couple of percents improvement (reduction) of *H* can not seem much, it can aid the end user's decision making process when choosing a soft-magnetic core.

## References

/1/ International standard IEC60404-2, Methods of measurement of magnetic, electrical and physical properties of magnetic sheet and strip, 1996.

/2/ Deutsche Norm DIN 50 460, Bestimmung der magnetischen Eigenschaften von weich-magnetischen Werkstoffen, 1988.

/3/ E. Carminati, A. Ferrero, A Virtual Instrument for the Measurement of the Characteristics of Magnetic Materials, *IEEE Trans. Instrum. Meas.*, vol. 41, pp. 1005 - 1009, Dec 1992.

/4/ A. Boglietti, P. Ferraris, M. Lazzari, M. Pastorelli, F. Profumo, New Power Supply Method for Soft Magnetic Material Characterization at High Flux Density Values, *IEEE Trans. Magn.*, vol. 28, pp. 2459 - 2461, Sep 1992.

/5/ L. D'Alessandro, A. Ferrero, A Method for the Determination of the Parameters of the Hysteresis Model of Magnetic Materials, *IEEE Trans. Instrum. Meas.*, vol. 43, pp. 599 - 605, Aug 1994.

/6/ J. Buck J, Automatic Hysteresisgraph Speeds Accurate Analysis of Soft Magnetic Materials, *PCIM*, February 2000, on-line version at: http://www.walkerldjscientific.com/buck.pdf

/7/ M. Petkovsek, J. Nastran, P. Zajec, F. Pavlovcic, D. Voncina, Soft-magnetic ring core measuring system with a decreased number of primary and secondary winding turns, *IEEE Trans. Instrum. Meas.*, vol. 53, No. 2, 2004, pp. 444 - 447.

/8/ N. M. Oldham, O. B. Laug, B. C. Waltrip, Digitally Synthesized Power Calibration Source, *IEEE Trans. Instrum. Meas.*, vol. IM-36, No. 1, pp. 341 - 346, June 1987.

/9/ H. Lavric, D. Voncina, P. Zajec, F. Pavlovcic, J. Nastran, A precision hybrid amplifier for voltage calibration systems, *Inf. MIDEM*, vol. 34, No. 1, 2004, pp. 37 - 42.

/10/ T. Yokoyama, A. Kawamura, Disturbance Observer Based Fully Digital Controlled PWM Inverter for CVCF Operation, *IEEE Trans. Power Electron.*, vol. 9, No. 5, pp. 473 - 480, Sep.1994.

/11/ C. G. Anwar, M. Tomizuka, Plug in Repetitive Control for Industrial Robotic Manipulators, *Proc. IEEE Int. Conf. Robot. Automat.*, pp. 1970 - 1975, May 1990.

/12/ A. Gubisch, P. L. Lualdi Jr., P. N. Miljanic, J. L. West, Power Calibrator Using Sampled Feedback for Current and Voltage, *IEEE Trans. Instrum. Meas.*, vol. 46, No. 2, pp. 403 - 407, Apr. 1997.

/13/ C. Rech, H. Pinheiro, H. A. Gründling, H. L. Hey, J. R. Pinheiro, Comparison of Digital Control Techniques With Repetitive Integral Action for Low Cost PWM Inverters, *IEEE Trans. Power Electron.*, vol. 18, No. 1, pp. 401 - 410, Jan. 2003.

/14/ K. Zhang, Y. Kang, J. Chen, Direct Repetitive Control of SPWM Inverter for UPS Purpose, *IEEE Trans. Power Electron.*, vol. 18, No. 3, pp. 784 - 792, May 2003.

/15/ Y. Ito, S. Kawauchi, Microprocessor Based Robust Digital Control for UPS with Three-Phase PWM Inverter, *IEEE Trans. Power Electron.*, vol. 10, No. 2, pp. 196 - 204, Mar. 1995.

*mag. Gorazd Modrijan, univ. dipl. inž. el.*
*as. dr. Marko Petkovšek, univ. dipl. inž. el.*
*doc. dr. Peter Zajec, univ. dipl. inž. el.*
*izr. prof. dr. Danijel Vončina, univ. dipl. inž. el.*

*Laboratorij za močnostno elektroniko in regulacijsko tehniko*
*Univerza v Ljubljani, Fakulteta za elektrotehnko*
*Tržaška cesta 25, 1000 Ljubljana, Slovenija*
*e-mail: gorazd.modrijan@fe.uni-lj.si,*
*marko.petkovsek@fe.uni-lj.si,*
*peter.zajec@fe.uni-lj.si,*
*voncina@fe.uni-lj.si*
*tel: +386 1 47 68 466, fax: +386 1 47 68 487*

*Prispelo (Arrived): 14. 02. 2006; Sprejeto (Accepted): 29. 05. 2006*